

# Peptide Mimetic of the Third Cytoplasmic Loop of the PTH/PTHrP Receptor

Dale F. Mierke,<sup>\*,†,‡</sup> Miriam Royo,<sup>§</sup> Maria Pellegrini,<sup>‡</sup> Hongmao Sun,<sup>‡</sup> and Michael Chorev<sup>§</sup>

Contribution from the Gustaf H. Carlson School of Chemistry, Clark University, 950 Main Street, Worcester, Massachusetts 01610, Department of Pharmacology & Molecular Toxicology, University of Massachusetts, Medical Center, 55 Lake Avenue North, Worcester, Massachusetts 01655, and Division of Bone & Mineral Metabolism, Beth Israel Hospital, Harvard Medical School, 330 Longwood Ave, Boston, Massachusetts 02215

Received February 12, 1996<sup>⊗</sup>

**Abstract:** The third cytoplasmic loop of seven transmembrane helix receptors is important both for the coupling to and activation of the heterotrimeric G-protein. Here, the structural characterization of two peptides containing the sequence of the putative third cytoplasmic loop of the parathyroid hormone/parathyroid hormone related peptide receptor in aqueous solution and in the presence of micelles is presented. The 27-amino acid peptide has been examined both in a linear form and cyclized with a linker of 8 methylenes designed to maintain a distance of 12 Å between the N- and C-termini, modeling the distance observed between transmembrane  $\alpha$ -helices in bacteriorhodopsin. In aqueous solution both peptides are relatively unstructured. In contrast, in the presence of sodium dodecylsulfate micelles the linear peptide adopts a well-defined extended conformation with approximately 30%  $\alpha$ -helix. The cyclic peptide possesses an N-terminal, ten amino acid  $\alpha$ -helical domain followed by seven amino acids which protrude out in a well-defined loop. These results indicate the importance of the membrane environment and the role of the structural constraint achieved by cyclization; the octamethylene linker restricts the peptide to conformations possible while attached to transmembrane helices V and VI thus mimicking the conformation of the loop in the native receptor.

## Introduction

Parathyroid hormone (PTH) regulates mineral metabolism and bone turnover by activating specific receptors located on osteoblastic and renaltubular cells, while PTH-related peptide (PTHrP), which has partial sequence homology to PTH, is associated with the syndrome of humoral hypercalcemia of malignancy.<sup>1–3</sup> Both PTH and PTHrP bind to the same receptor,<sup>4–7</sup> which is a member of a recently recognized subfamily of G-protein coupled receptors that includes the receptors for hormones such as secretin, glucagon, glucagon-

like peptide, calcitonin, growth hormone-releasing hormone, and vasoactive intestinal polypeptide.<sup>8–15</sup> This subclass of receptors show a high degree of homology (30–60%), a relatively long amino-terminal extracellular domain with multiple potential N-glycosylation sites, and a highly conserved pattern of eight cysteines in the amino-terminal and the first and second extracellular loops. Recently an alternative receptor subtype, PTH2, has been identified which has approximately 70% homology with the PTH/PTHrP receptor. However, the PTH2 receptor is activated only by PTH, not by PTHrP.<sup>16</sup> The function of the PTH2 receptor which is most abundant in the brain and pancreas awaits further study.

From chimeric studies of the PTH/PTHrP receptor the extracellular portion of the receptor has been shown to be important for peptide binding.<sup>17</sup> The binding of the hormone

\* Author to whom correspondence should be addressed.

† Clark University.

‡ University of Massachusetts, Medical Center.

§ Harvard Medical School.

⊗ Abstract published in *Advance ACS Abstracts*, September 1, 1996.

(1) Suva, L. J.; Winslow, G. A.; Wettenhall, R. E.; Hammonds, R. G.; Moseley, J. M.; Diefenbach-Jagger, H.; Rodda, C. P.; Kemp, B. E.; Rodriguez, H.; Chen, E. Y.; Hudson, P. J.; Martin, T. J.; Wood, W. I. *Science* **1987**, *237*, 893–896.

(2) Mangin, M.; Webb, A. C.; Dreyer, B. E.; Posillico, J. T.; Ikeda, K.; Weir, E. C.; Stewart, A. F.; Bander, N. H.; Milstone, L.; Barton, D. E.; Francke, U.; Broadus, A. E. *Proc. Natl. Acad. Sci. U.S.A.* **1988**, *85*, 597–601.

(3) Strewler G. J.; Stern P. H.; Jacobs J. W.; Eveloff J.; Klein R. F.; Leung S. C.; Rosenblatt M.; Nissenson R. A. *J. Clin. Invest.* **1987**, *80*, 1803–1807.

(4) Jüppner, H.; Abou-Samra, A.-B.; Freeman, M.; Fong, X. F.; Schipani, E.; Richards, J.; Kolakowski, L. F., Jr.; Hock, J.; Potts, J. T., Jr.; Kronenberg, H. M.; Segre, G. V. *Science* **1991**, *254*, 1024–1026.

(5) Abou-Samra, A.-B.; Jüppner, H.; Force, T.; Freeman, M. W.; Kong, X.-F.; Schipani, E.; Urena, P.; Richards, J.; Bonventre, J. V.; Potts J. T., Jr.; Kronenberg, H. M.; Segre, G. V. *Proc. Natl. Acad. Sci. U.S.A.* **1992**, *89*, 2732–2736.

(6) Schipani, E.; Karga, H.; Karaplis, A. C.; Potts, J. T., Jr.; Kronenberg, H. M.; Segre, G. V.; Abou-Samra, A.-B.; Jüppner, H. *Endocrinology* **1993**, *132*, 2157–2165.

(7) Adams, A. E.; Chorev, M.; Rosenblatt, M.; Suva, L. J. *J. Bone Miner. Res.* **1993**, *8* (Suppl 1), S195.

(8) Jelinek, L. J.; Lok, S.; Rosenberg, G. B.; Smith, R. A.; Grant, F. J.; Biggs, S.; Bensch, P. A.; Kuijper, J. L.; Sheppard, P. O.; Sprecher, C. A.; O'Hara, P. J.; Foster, D.; Walker, K. M.; Chen, L. H. J.; McKernan, P. A.; Kindsvogel, W. *Science* **1991**, *259*, 1614–1616.

(9) Thorens, B. *Proc. Natl. Acad. Sci. U.S.A.* **1992**, *89*, 8641–8645.

(10) Li, H. Y.; Harris, T. L.; Flannery, M. S.; Aruffo, A.; Kaji, E. H.; Gorn, A.; Kolakowski, L. F., Jr.; Lodish, H. F.; Goldring, S. R. *Science* **1991**, *254*, 1022–1024.

(11) Ishihara, T.; Nakamura, S.; Kaziro, Y.; Takahashi, T.; Takahashi, K.; Nagata, S. *EMBO J.* **1991**, *10*, 1635–1641.

(12) Ishihara, T.; Shigemoto, R.; Mori, K.; Takahashi, K.; Nagata, S. *Neuron* **1992**, *8*, 811–819.

(13) Mayo, K. E. *Mol. Endocrinol.* **1992**, *6*, 1734–1744.

(14) Gaylinn, B. D.; Harrison, J. K.; Zysk, J. R.; Lyons, C. E.; Lynch, K. R.; Thorner, M. O. *Mol. Endocrinol.* **1993**, *7*, 77–84.

(15) Sgre, G. V.; Goldring, S. R. *Trends Endocrinol. Metab.* **1993**, *4*, 309–314.

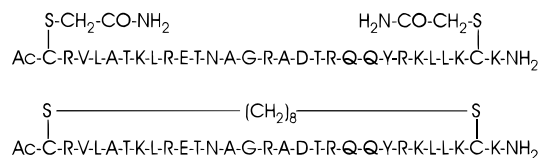
(16) Usdin, T. B.; Gruber, C.; Bonner, T. I. *J. Biol. Chem.* **1995**, *270*, 15455–15458.

(17) Jüppner, H.; Schipani, E.; Bringham, F. R.; McClure, I.; Keutmann, H. T.; Potts, J. T., Jr.; Kronenberg, H. M.; Abou-Samra, A. B.; Segre, G. V.; Gardella, T. J. *Endocrinology* **1994**, *134*, 879–884.

stimulates multiple signal transduction pathways that include cAMP, inositol phosphate, and calcium and activation of both protein kinase A and C.<sup>5</sup> All of these actions are mediated by the heterotrimeric G-proteins G<sub>s</sub>, G<sub>11</sub>, or G<sub>q</sub>. The peptide binding to the receptor induces a conformational change in the G-protein which exposes the guanyl-nucleotide binding site leading to rapid exchange of GDP for GTP.<sup>18,19</sup> The now activated G-protein then acts as an effector, or activates other effector proteins, leading to the signal. The mechanism by which receptor occupation by the agonist initiates the activation of the G-protein is of great pharmacological interest.

From studies of the  $\beta$ -adrenergic receptor, the third cytoplasmic loop (I3) has been shown to be determinant in the coupling with the G-protein; mutations or chimeric replacement in I3 of the receptor alter the association of the G-protein, producing receptors that display modified or a lack of selectivity for their endogenous G-proteins.<sup>20–22</sup> The third loop is also important for activation; synthetic peptides containing portions of the third loop of the  $\beta$ -adrenergic receptor have been shown to activate G-proteins.<sup>23,24</sup> Structure predictions for these peptides show a high propensity for  $\alpha$ -helices, although a direct correlation between  $\alpha$ -helical structures and activation of the G-protein is not evident.<sup>25</sup>

In this study we undertake the conformational investigation of the I3 of the PTH/PTHrP receptor by <sup>1</sup>H NMR and computer simulations. The peptide has been examined in two forms, linear and cyclic, incorporating eight methylenes between the side-chain sulfurs of two cysteine residues located at the N- and C-termini of the peptide.



The cyclic peptide has been designed to allow a distance of 12 Å between the termini, and therefore mimic the native state in which the peptide is attached to the cytoplasmic ends of transmembrane  $\alpha$ -helices (TM) V and VI. Both the linear and cyclic peptides have been examined in aqueous solution and in the presence of sodium dodecylsulfate (SDS) micelles, a mimetic for the membrane environment.<sup>26</sup> The results from this study provide insight into the possible conformational changes which the I3 may undergo upon ligand binding to the receptor.

## Experimental Procedures

**Materials.** The peptides were prepared on *p*-methylbenzhydrylamine hydrochloride resin obtained from Applied Biosystems (Foster City, CA). The Boc-amino acids and the reagents used for synthesis were also obtained from Applied Biosystems. The Fmoc-Cys(Trt)-OH was obtained from Bachem-California (Torrance, CA). Hydrogen

(18) Conklin, B. R.; Bourne, H. R. *Cell* **1993**, *73*, 631–641.

(19) Neer, E. J. *Cell* **1995**, *80*, 249–257.

(20) Wong, S. K. F.; Parker, E. M.; Ross, E. M. *J. Biol. Chem.* **1990**, *265*, 6219–6224.

(21) Cotecchia, S.; Ostrowski, J.; Kjelsberg, M. A.; Caron, M. G.; Lefkowitz, R. J. *J. Biol. Chem.* **1992**, *267*, 1633–1639.

(22) Wong, S. K. F.; Ross, E. M. *J. Biol. Chem.* **1994**, *269*, 18968–18976.

(23) Strader, C. D.; Fong, T. M.; Tota, M. R.; Underwood, D.; Dixon, R. A. F. *Annu. Rev. Biochem.* **1994**, *63*, 101–132.

(24) Okamoto, T.; Murayama, Y.; Hayashi, Y.; Inagaki, M.; Ogata, E.; Nishimoto, I. *Cell* **1991**, *67*, 723–730.

(25) Voss, T.; Wallner, E.; Czernilofsky, A. P.; Freissmuth, M. *J. Biol. Chem.* **1993**, *268*, 4637–4642.

(26) (a) McDonnell, P. A.; Opella, S. J. *J. Magn. Reson. B* **1993**, *102*, 120–126. (b) Kallick, D. A.; Tessmer, M. R.; Wtts, C. R.; Li, C.-Y. *J. Magn. Reson. B* **1995**, *109*, 60–65.

fluoride (HF) was purchased from Matheson (Secaucus, NJ). DIEA, piperidine, dithiothreitol, 1,8-dibromooctane, trifluoroacetic acid (TFA, spectroscopic grade), and iodoacetamide were from Aldrich (Milwaukee, WI). The HF reaction was carried out in a Type 1B apparatus from Peninsula Laboratories (Belmont, CA). Dichloromethane, NMP, DMF and acetonitrile were from Baxter (Muskegon, MI). RP-HPLC columns used in analytical and preparative modes were Vydac protein/peptide C18, 300 Å (0.46 × 15 cm, 5 μm) from The Separations Group (Hesperia, CA) and Vydac protein/peptide C18, 300 Å (2.2 × 25 cm, 15–20 μm) from Millipore (Milford, MA), respectively. The solvent system employed consisted of 0.1% (v/v) TFA in H<sub>2</sub>O (A) and 0.1% (v/v) TFA in acetonitrile (B). The separation was monitored at 220 nm.

**Solid-Phase Peptide Synthesis.** The peptides were synthesized by solid-phase methodology on a ABI 430A peptide synthesizer employing *p*-methylbenzhydrylamine resin (0.25 mmol scale, *f* = 0.81 mmol/g). All the couplings were carried out with the hydroxybenzotriazole method using diisopropylcarbodiimide as the coupling reagent. The synthesis was carried out by NMP-HOBt-t-BOC protocols.<sup>27</sup> Systematic double coupling was employed for residues 2, 3, 8, 9, 10, 11, and 18 while a modified cycle (extended coupling in DMSO for 32 m instead of 16 m) was used for residue 17. The capping via acetylation, at the end of each coupling cycle, was carried out on the ABI 430A synthesizer. The N-terminal cysteine was introduced (cyclic peptide) via manual coupling employing Fmoc-Cys(Trt)-OH and using the same coupling method as used in the automatic synthesis.

**Cyclic Peptide.** The Fmoc group was deprotected with piperidine–DMF (2:8) (1 × 1 min, 1 × 15 min). After washings with DMF (3 × 1 min) and CH<sub>2</sub>Cl<sub>2</sub> (3 × 1 min) the free amino terminal group was acetylated by treatment with a solution of Ac<sub>2</sub>O–CH<sub>2</sub>Cl<sub>2</sub> (1:9 v/v) for 1 h. The octamethylene chain was introduced on the solid phase by alkylating the N-terminal cysteine with 1,8-dibromooctane after Trt deprotection. This was carried out as follows: washes with CH<sub>2</sub>Cl<sub>2</sub> (5 × 30 s), treatment with TFA–H<sub>2</sub>O (9:1) (1 × 1 min, 1 × 15 min), treatment with TFA–CH<sub>2</sub>Cl<sub>2</sub>–H<sub>2</sub>O (9:0.5:0.5) (1 × 1 min, 1 × 15 min) and with TFA–phenol–H<sub>2</sub>O (9:0.5:0.5) (1 × 1 min, 1 × 15 min), and final washes with CH<sub>2</sub>Cl<sub>2</sub> (5 × 30 s) and DMF (5 × 30 s). The resin was suspended in 10 mL of DMF, 69 μL of Br-(CH<sub>2</sub>)<sub>8</sub>-Br (1.5 equiv, 0.37 mmol) and 43 μL of DIEA (1 equiv, 0.25 mmol) was added, followed by shaking overnight. The resin was washed with DMF (5 × 30 s) and DCM (5 × 30 s). The peptide was cleaved from the resin and deprotected by treatment with HF–anisole (19:1 v/v) for 75 min at 0 °C. The major peak (*k'* = 5.95) was collected by analytical HPLC employing a linear gradient of 20–50% B in A in 30 min at a flow rate of 1 mL/min and characterized by FAB-MS (MW calcd 3652.02; [M + H]<sup>+</sup> 3654.5).

The crude peptide (316 mg) from the cyclic precursor (86 μmol) was dissolved in 880 mL of H<sub>2</sub>O and 8.6 mL of DIEA was added to the reaction mixture. The reaction was monitored by analytical HPLC (see conditions above). After 8 h the reaction was stopped by addition of AcOH–H<sub>2</sub>O (50:50, v/v) to reach a pH of 4. The crude cyclic peptide obtained after removal of solvent under reduced pressure was dissolved in H<sub>2</sub>O and purified by preparative HPLC employing a linear gradient of 20–25% (v/v) B in A in 75 min at a flow rate of 70 mL/min. A 20.1-mg yield of pure cyclic peptide (5.6 μmol, yield 6.5%) was obtained. The purity and composition of the cyclic peptide was analyzed by analytical HPLC (*k'* = 3.65 (see conditions above) and amino acid analysis (calcd): 63% peptide content; Asx (Asp and Asn) 2.21 (2), Thr 2.66 (3), Glx (Glu and Gln) 3.06 (3), Gly 1.07 (1), Ala 3.02 (3), Val 0.89 (1), Leu 4.04 (4), Tyr 1.08 (1), Lys 3.97 (4), Arg 4.9 (5), Cys not determined. FAB-MS analysis: MW calcd 3572; [M + H]<sup>+</sup> 3572.0.

**Linear Peptide.** The precursor of the linear peptide was cleaved from the resin and deprotected by treatment with HF–anisole (19:1 v/v) for 75 min at 0 °C. Crude peptide (900 mg, 260 μmol) was treated with 8 equiv of dithiothreitol in aqueous solution for 15 min and purified by preparative HPLC employing a linear gradient of 10–40% B in A in 90 min at a flow rate of 70 mL/min. A 310-mg yield of pure reduced

(27) Geiser, T.; Beilan, T.; Berogt, B. J.; Offeson, K. M. Automation of solid-phase peptide synthesis. In *Macromolecular sequencing and synthesis: Selected methods and applications*; Schlesinger, D. H., Ed.; Alan R. Liss: New York, 1988; pp 199–218.

peptide (89.5  $\mu\text{mol}$ , 34% purification yield) was obtained. The purity and composition was confirmed by analytical HPLC  $k' = 6.23$ , employing a linear gradient of 15–45% (v/v) B in A in 30 min and amino acid analysis: 74% peptide content, Asx (Asp and Asn) 1.83 (2), Thr 2.63 (3), Glx (Glu and Gln) 2.86 (3), Gly 0.83 (1), Ala 2.55 (3), Val 0.87 (1), Leu 3.56 (4), Tyr 0.89 (1), Lys 3.47 (4), Arg 4.38 (5), Cys (2) not determined. FAB-MS analysis: MW calcd 3462.121;  $[M + H]^+ 3461.8$ . Reduced precursor of the linear peptide (284 mg; 82  $\mu\text{mol}$ ) was dissolved in 10 mL of 0.05 M sodium acetate buffer (pH 5.5) under  $\text{N}_2$ . A solution of 2.3 equiv of  $\text{ICH}_2\text{CONH}_2$  (35.2 mg, 0.19 mmol), dissolved in 100  $\mu\text{L}$  of 0.05 M sodium acetate buffer, was added in four portions. After 7.5 h the reduced product was consumed and the reaction was stopped by addition of  $\text{AcOH-H}_2\text{O}$  50% to reach pH 3–4. The linear peptide was purified by preparative HPLC employing a linear gradient of 15–40% (v/v) B in A in 125 min at a flow rate of 70 mL/min. A yield of 170 mg of pure linear peptide (47.5  $\mu\text{mol}$ , yield 58%) was obtained. The purity and composition of the linear peptide was analyzed by analytical HPLC  $k' = 5.66$  employing a linear gradient of 15–45% B in A in 30 min and amino acid analysis: 61% peptide content; Asx (Asp and Asn) 2.00 (2), Thr 2.43 (3), Glx (Glu and Gln) 3.09 (3), Gly 1.05 (1), Ala 2.97 (3), Val 0.89 (1), Leu 3.96 (4), Tyr 0.95 (1), Lys 4.08 (4), Arg 5.7 (5), Cys (2) not determined. FAB-MS analysis of the linear peptide gave the correct molecular weight (MW calcd 3576.7;  $[M + H]^+ 3576.7$ ;  $[M - \text{CH}_2\text{CONH}_2 + H]^+ 3518.4$ ).

**Circular Dichroism.** CD measurements were performed on a spectropolarimeter at 25  $^\circ\text{C}$  in a thermostated cell holder. Quartz cells with optical path length of 0.1 cm were used. Solutions used for the CD measurements were prepared by dissolving weighted quantities of peptides in water or water/SDS at a pH of 5.4. Solute concentrations ( $3.0 \times 10^{-5}$  M) were calculated using the apparent molecular weight of each sample found by amino acid analysis. Mean residue ellipticities,  $[\theta]$  ( $\text{deg cm}^2 \text{dmol}^{-1}$ ), were calculated in the usual fashion using the mean residue weight calculated from the peptide molecular weights. Each spectrum is the average of two scans. No curve smoothing was used.

**Nuclear Magnetic Resonance.** Samples (2 mM) for  $^1\text{H}$  NMR spectroscopy were prepared by dissolving the peptides in 700  $\mu\text{L}$  of either 90%  $\text{H}_2\text{O}/10\%$   $^2\text{H}_2\text{O}$  or 100%  $^2\text{H}_2\text{O}$  (99.98%  $^2\text{H}$ ). The micellar samples contained 220 mM of perdeuterated sodium dodecylsulfate ( $\text{SDS-}^2\text{H}_{25}$ , MSD Isotopes, Montreal). The pH was adjusted to 5.4.

NMR experiments were performed on a Varian Unity 500-MHz spectrometer. 2D-TOCSY, NOESY, and P. E. COSY spectra were recorded at 25, 35, and 45  $^\circ\text{C}$  in the phase sensitive mode. A spectral width of 5000 Hz was used and 256–320 complex points in  $t_1$  and 4K points in  $t_2$  were collected. The water peak was suppressed by presaturation during the recycle delay. The TOCSY experiment employed an MLEV-17 sequence with mixing times of 20 and 60 ms and 2 ms trim pulses. NOESY data were obtained using mixing times of 75, 125, 175, and 250 ms. Spectra were processed using VNMR (Varian) or FELIX (Biosym, Inc.). Chemical shifts were referenced to an external reference.

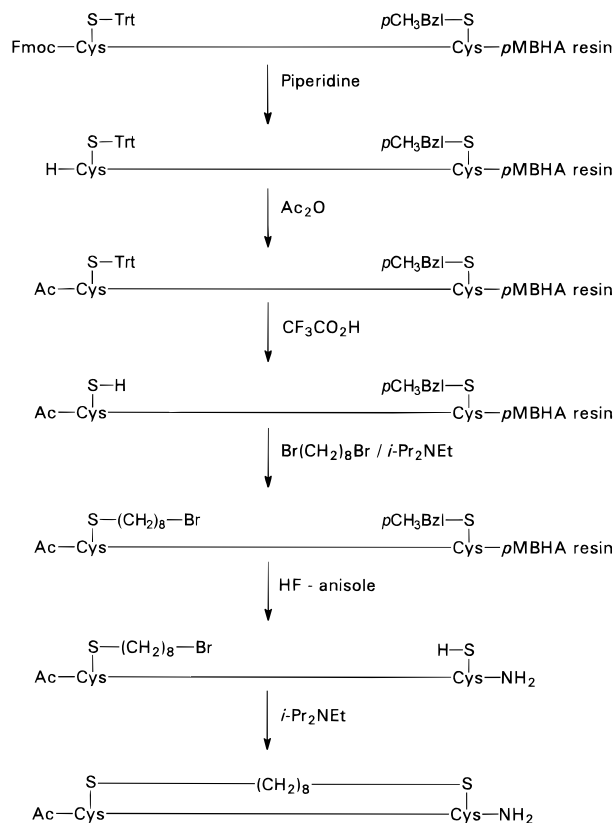
A list of distance constraints was generated by integration of the cross-peaks in the NOESY spectrum using the two-spin approximation and geminal protons as a reference (set to 1.8  $\text{\AA}$ ). No evidence of second-order effects (spin-diffusion) was observed up to a mixing time of 250 ms (i.e., cross-peak buildup rates were approximately linear). The upper and lower distance restraints were created by addition and subtraction of 10% of the calculated distance. NOEs from both  $\text{H}_2\text{O}$  and  $^2\text{H}_2\text{O}$  samples were utilized; spectra using the latter were important for NOEs involving aliphatic and aromatic proton resonances. Only NOEs which produce distance restraints tighter than those generated from the molecular constitution (holomeric distances) were used in the structure calculations and considered in the discussion below.

The distance geometry (DG) calculations were carried out with a home-written program utilizing the random metrization algorithm of Havel.<sup>28</sup> The structures were first embedded in four dimensions and a simulated annealing protocol which utilizes the distance matrix as a penalty function was run following procedures previously published.<sup>29,30</sup>

(28) Havel, T. F. *Prog. Biophys. Mol. Biol.* **1991**, *56*, 33–56.

(29) Jahnke, W.; Mierke, D. F.; Beress, L.; Kessler, H. *J. Mol. Biol.* **1994**, *240*, 445–458.

### Scheme 1



The resulting structures were then reduced to three dimensions using metrization and the simulated annealing procedure repeated. The resulting structures were energy minimized using the Discover force field within the Insight II molecular modeling program (Biosym, Inc.).

### Results

Introduction of the octamethylene bridge between the two cysteines side chains was carried out in a stepwise manner combining solid- and solution-phase S-alkylation steps (see Scheme 1). Introduction of Fmoc-Cys(S-Trt) at the last coupling step allowed selective removal of the  $\text{N}_\alpha$ -Fmoc group followed by the N-acylation of the free amino terminus. While on the resin, deprotection of the S-Trt of the N-terminal cysteine was followed by S-alkylation. Cleavage from the resin with concomitant removal of side chain protecting groups exposed the thiol group of the C-terminal cysteine and allowed for the second S-alkylation, resulting in the ring formation. Purity of final peptides exceeded 98% as assessed by analytical HPLC. Amino acid analysis and FAB-MS analyses confirmed the structural integrity of the final products.

The CD spectra of the linear and cyclic peptides in benign aqueous solution are consistent with unordered structures. Therefore, the structure of the peptides in benign aqueous solution will not be discussed further. In the presence of SDS micelles both of the peptides show a percentage of  $\alpha$ -helix: approximately 30% for the linear and 20% for the cyclic peptide. A comparison of the CD spectra obtained for the linear peptide in aqueous solution and in the presence of SDS micelles is shown in Figure 1.

All  $^1\text{H}$ -NMR resonances of the linear and cyclic peptides in the presence of micelles were assigned using the standard two-step procedure of spin system identification, via TOCSY and COSY spectra, followed by the sequential assignment, from

(30) Mierke, D. F.; Kurz, M.; Kessler, H. *J. Am. Chem. Soc.* **1994**, *116*, 1042–1049.

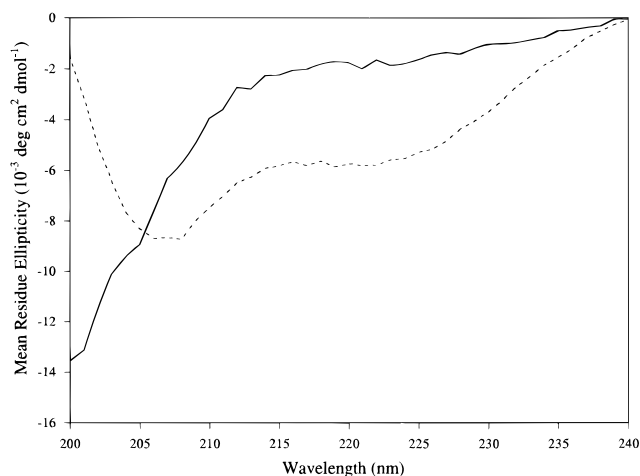


**Figure 1.** Circular dichroism spectra of the linear peptide containing the I3 of the PTH/PTHrP receptor in aqueous solution (solid line) and in the presence of SDS micelles (dotted line). The spectra are the average of two scans collected at 25 °C with no line smoothing.

NOESY spectra.<sup>31</sup> The difference between the observed chemical shift and that for an unordered structure can provide tentative information regarding the presence of secondary structure. Although the information content is enhanced with inclusion of heteronuclei (<sup>15</sup>N, <sup>13</sup>C), some general trends can be observed solely using <sup>1</sup>H resonances. In Figure 2, the difference of the chemical shift of the  $\alpha$  protons, H $\alpha$ , observed by us and reported by Wüthrich<sup>31</sup> is illustrated. The upfield shift of the protons of the N-terminus is consistent with an  $\alpha$ -helix. The small differences in chemical shifts for the residues of the middle of the peptide may indicate flexibility. However, care must be used since the chemical shifts could be altered due to interaction with the micelle and the reference chemical shifts are for those of a random-coil in water; any conclusions regarding conformation must be further substantiated by NOEs.

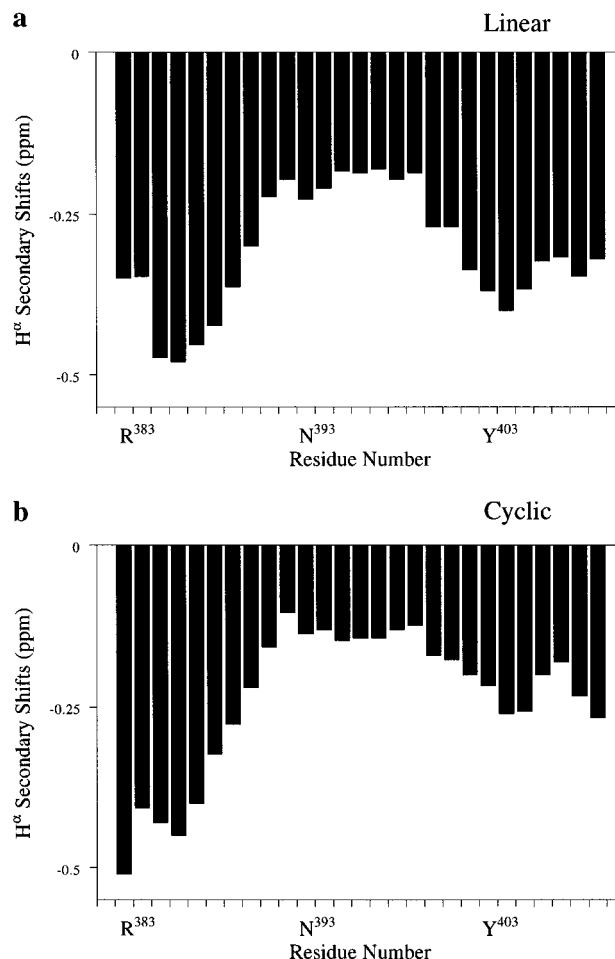
In Figure 3, an expanded portion of the amide region of a NOESY spectrum of the cyclic peptide illustrating the large number of HN(*i*)-HN(*i*+1) NOEs is given. The consecutive string of strong NOEs observed for the N-terminus is consistent with an  $\alpha$ -helix. In addition, the fingerprint region contains a large number of *i*, *i*+3 NOEs for the N-terminal residues. These NOEs indicating the presence of an  $\alpha$ -helix are observed for both the linear and cyclic peptide. The distribution of inter- and intraresidue NOEs observed for both peptides is illustrated in Figure 4. A slightly larger number of informative NOEs have been observed for the cyclic analog (287 NOEs) than for the linear peptide (266 NOEs). Both peptides have an unusually large number of NOEs for Tyr<sup>403</sup>.

The DG calculations were repeated 100 times for both the linear and cyclic peptides, producing ensembles of 92 and 69 low-energy structures, respectively. The average over these ensembles of structures completely fulfills the upper and lower distance restraints; there are no distance violations greater than 0.2 Å when using the ensemble average, and no violations greater than 0.3 Å are observed for individual structures.

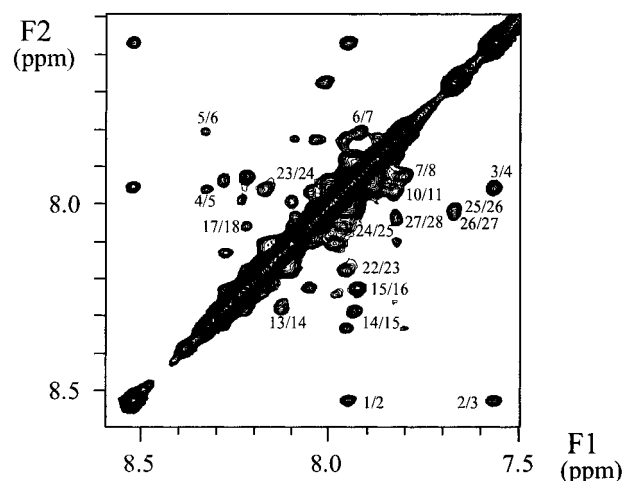
One manner to examine the range of conformations within an ensemble of structures is the dihedral angle order parameter, which ranges from 1.0, indicating that the dihedral angle is identical for all structures (complete order), to a value of 0.0, indicating no order.<sup>32</sup> The order parameters for the  $\phi$  and  $\psi$  dihedral angles (provided in supporting information) reveal a convergence of conformation in the N-terminal, twelve amino

(31) Wüthrich, K. *NMR of proteins and nucleic acids*; John Wiley, New York, 1986.

(32) Havel, T. F. *Biopolymers* **1990**, *29*, 1565–1585.



**Figure 2.** Difference in observed <sup>1</sup>H-NMR chemical shifts and those reported for unstructured peptides for the linear (a) and cyclic (b) peptide containing the I3 of the PTH/PTHrP receptor.



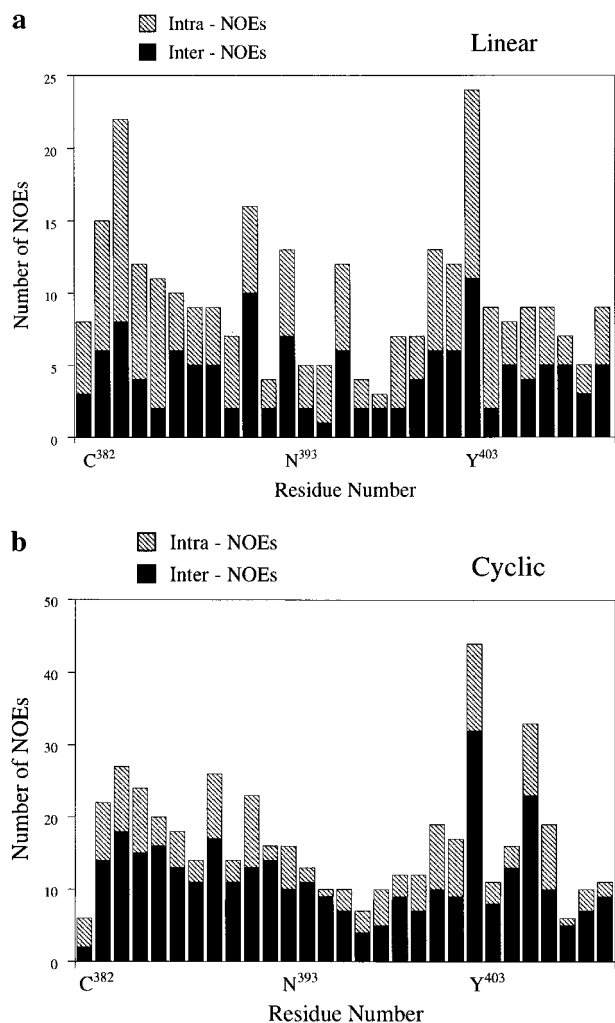


**Figure 4.** The distribution of intra- and interresidue NOEs for the linear (a) and cyclic (b) peptides containing the I3 of the PTH/PTHrP receptor.

C-terminus of the linear peptide there are a few *i, i+3* NOEs which are indicative of one turn of an  $\alpha$ -helix. These NOEs are not sufficient to produce the helix in every structure. This may be an indication of a nascent helix,<sup>33</sup> a helix that is present for only a short period of time or for only a small percentage of the ensemble of structures. The order parameters illustrate that the cyclic peptide is well ordered from residues 21–27 (Gln<sup>402</sup>–Lys<sup>408</sup>) with a flexible C-terminus. This region, structurally well-resolved, is centered about Tyr<sup>403</sup> and Leu<sup>406</sup>, both of which are involved in a large number of NOEs. In Figure 5, the NOEs observed for the cyclic peptide are displayed on one minimum energy structure taken from the ensemble of structures. The large density of NOEs in the N-terminal  $\alpha$ -helix and in the region about Tyr<sup>403</sup> are clearly illustrated.

## Discussion

The number of ligands which exert their activity through a membrane bound G-protein coupled receptor is steadily increasing. Although there are differences in binding sites with small ligands (e.g., catecholamines, norepinephrine, adenosine, epinephrine) binding within the transmembrane helices, while peptide ligands bind somewhere in the extracellular domain, the mode of action is similar; ligand binding leads to the activation of a G-protein.<sup>19,34,35</sup> Peptide fragments of several

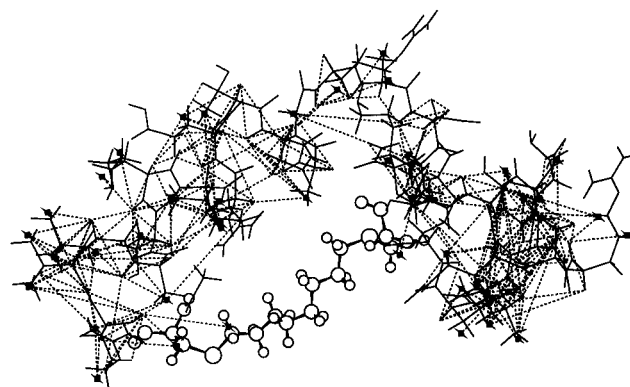


**Figure 5.** The NOEs observed for the cyclic peptide in the presence of SDS micelles are graphically illustrated on a minimum energy structure, chosen from the ensemble of acceptable structures. The NOEs are shown as dashed lines. The solid dots indicate pseudatoms for methyl groups and nondiastereotopically assigned methylene groups.

G-protein coupled receptors are reported to modulate receptor/G-protein coupling and/or to directly stimulate GDP-GTP exchange of G-proteins.<sup>36–45</sup> In many of these studies peptides derived from the third intracellular loop (I3) of the G-protein coupled receptors were identified as the major, but not the only, interacting domain with the G-proteins. An example is peptide Q a tetradecapeptide that corresponds to the carboxy-terminal region of I3 of the  $\alpha_{2a}$ -adrenergic receptor.<sup>38,41</sup> Peptide Q lowers binding affinity for radiolabeled agonist and activates the GTPase activity of a purified G-protein. Mutations in I3 result in constitutive activation of the thyrotropin,  $\alpha_{1b}$ - and  $\beta_2$ -adrenergic receptors<sup>46–48</sup> and modify signaling pathways of the thyrotropin (TSH) and  $\alpha_1$ -adrenergic receptors.<sup>49,50</sup> This suggests that the role of the unoccupied receptor is to inhibit the G-protein; upon ligand binding the heterotrimeric G-protein dissociates from the receptor and is therefore activated. In either case, it is clear that ligand binding must induce a conformational change of the cytoplasmic portion of the receptor, and most studies to date have implicated the I3 (although the second loop

(36) König, B.; Arende, A.; McDowell, J.; Hargrave, P. A.; Hofmann, K. P. *J. Proc. Natl. Acad. Sci. U.S.A.* **1989**, *86*, 6878–6882.

(37) Kahlert, M.; König, B.; Hofmann, K. P. *J. Biol. Chem.* **1990**, *265*, 18928–18932.

(38) Dalman, H. M.; Neubig, R. R. *J. Biol. Chem.* **1991**, *266*, 11025–11029.

(39) Nishimoto, I.; Ogata, E.; Okamoto, T. *J. Biol. Chem.* **1991**, *266*, 12747–12751.

(40) Münch, D.; Dees, C.; Hekman, M.; Palm, D. *Eur. J. Biochem.* **1991**, *198*, 357–364.

(41) Taylor, J. M.; Jacob-Mosier, G. G.; Lawton, R. G.; Neubig, R. R. *Peptides* **1994**, *15*, 829–834.

(42) Palm, D.; Münch, D.; Dees, C.; Hekman, M. *FEBS Lett.* **1989**, *254*, 89–93.

(43) Cheung, A. H.; Huang, R.-R. C.; Graziano, M. P.; Strader, C. D. *FEBS Lett.* **1991**, *279*, 277–280.

(44) Ikezu, T.; Okamoto, T.; Ogata, E.; Nishimoto, I. *FEBS Lett.* **1992**, *311*, 29–32.

(45) Yeagle, P. L.; Alderfer, J. L.; Albert, A. D. *Biochemistry* **1995**, *34*, 14621–14625.

(46) Parma, J.; Duprez, L.; Van Sande, J.; Cochaux, P.; Gervy, C.; Mockel, J.; Dumont, J.; Vassart, G. *Nature* **1993**, *365*, 649–651.

(47) Kjelsberg, M. A.; Cotecchia, S.; Ostrowski, J.; Caron, M. G.; Lefkowitz, R. J. *J. Biol. Chem.* **1992**, *267*, 1430–1433.

(48) Lefkowitz, R. J.; Cotecchia, S.; Samama, P.; Costa, T. *Trends Pharmacol. Sci.* **1993**, *14*, 303–307.

(49) Kosugi, S.; Okajima, F.; Ban, Y.; Hidaka, A.; Shenker, A.; Kohn, L. D. *J. Biol. Chem.* **1992**, *267*, 24153–24156.

(50) Cotecchia, S.; Ostrowski, J.; Kjelsberg, M. A.; Caron, M. G.; Lefkowitz, R. J. *J. Biol. Chem.* **1992**, *267*, 1633–1639.

(51) Trumpf-Kallmeyer, S.; Hoflack, J.; Bruinvels, A.; Hilbert, M. *J. Med. Chem.* **1992**, *35*, 3448–3462.

(52) Ji, I.; Ji, T. *J. Biol. Chem.* **1991**, *266*, 14953–14957.

(53) Kosugi, S.; Okajima, F.; Ban, T.; Hidaka, A.; Shenker, A.; Kohn, L. D. *J. Biol. Chem.* **1992**, *267*, 24153–24156.

(33) Dyson, J.; Wright, P. W. *J. Mol. Biol.* **1988**, *29*, 1565–1585.

(34) Coughlin, S. R. *Curr. Op. Cell Biol.* **1994**, *6*, 191–197.

(35) Baldwin, J. M. *Curr. Op. Cell Biol.* **1994**, *6*, 180–190.

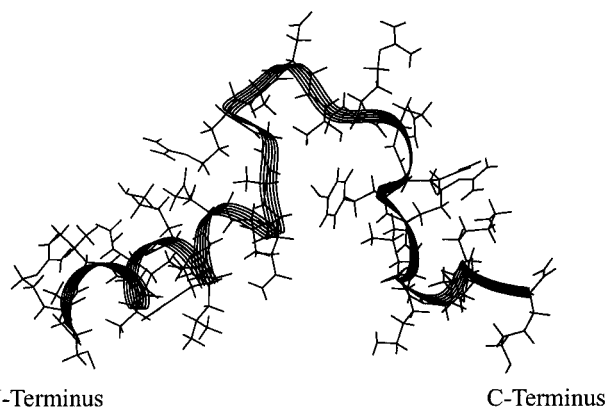


**Figure 6.** One indicative structure observed for the linear peptide containing the I3 of the PTH/PTHrP receptor in the presence of SDS micelles. The peptide backbone is illustrated as a ribbon.

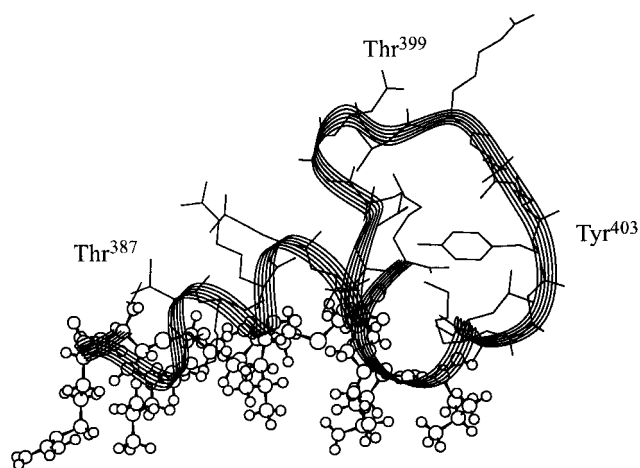


**Figure 7.** One low-energy structure of the cyclic peptide containing the I3 of the PTH/PTHrP receptor in the presence of SDS micelles. The amino acids believed to be interacting with the surface of the micelle are indicated as ball-and-stick.

and C-terminal domain of the receptor may play a role in the association and activation of the G-protein).<sup>51–53</sup> In an effort to define the conformational changes possible upon ligand binding, we have undertaken the structural investigation of the I3 of the PTH/PTHrP G-protein coupled receptor using CD, NMR, and computer simulations.

Both the linear and cyclic peptides show no evidence of preferred structure in aqueous solution as evidenced from both CD and NMR analysis. In the presence of micelles the linear peptide adopts an extended conformation, dominated by the N-terminal  $\alpha$ -helix. In Figure 6, a representative structure of the linear peptide is shown. Under identical conditions the cyclic peptide assumes a folded conformation which includes a shorter N-terminal  $\alpha$ -helix (see Figure 7). A helix has been postulated to be necessary for activation of G-proteins.<sup>23,43,54</sup> Mastoparan, an amphiphilic cationic  $\alpha$ -helical peptide isolated from bee venom activates G-proteins by enhancing the exchange of GDP and GTP,<sup>54</sup> although the presence of a helix is not the only requirement for activation.<sup>25</sup>

An important feature of the peptides examined here is the distance between the termini, where the cytoplasmic loop would normally attach to the membrane-spanning  $\alpha$ -helices TM-V and -VI of the receptor. The average distance between the terminal residues of the linear peptide is 28 Å, with distances ranging from 16 to 39 Å (the next shortest end-to-end distance is 23 Å, the structure shown in Figure 6 has a distance of 28 Å). The

range of distances observed is a result of the high flexibility of the middle portion of the peptide, directly after the N-terminal  $\alpha$ -helix. Since the distance between the transmembrane  $\alpha$ -helices, based on the structure of bacteriorhodopsin, is no greater than 15 Å, most of the low-energy conformations observed for the linear peptide cannot be adopted while a part of the intact receptor. These findings clearly illustrate the importance of the octamethylene bridge utilized in this investigation. It is vital for the design of a model peptide representing the I3 of the PTH/PTHrP receptor to eliminate (or at least minimize) conformations which are not possible in the intact receptor.

The addition of the terminal cysteine residues and the octamethylene linker was designed to keep the peptide termini at an average distance of 12 Å. The octamethylene linker is not rigid and therefore there will be variations in the end-to-end distance. In fact, the average distance between the termini of the cyclic peptide in the ensemble of structures is 13 Å, ranging from 9.8 to 16 Å. Similar to the linear peptide there is a well-defined  $\alpha$ -helix at the N-terminus followed by a flexible domain. Interestingly the C-terminal portion of the cyclic analog in the presence of SDS micelles is well-ordered, with a large number of NOEs in this region, mainly involving Tyr<sup>403</sup> and Leu<sup>406</sup>, with 44 and 32 NOEs involving these residues, respectively. Although there is no evidence of regular secondary structural elements in this region, the average, pairwise root-mean-square deviation of the backbone heavy atoms of the region from Arg<sup>400</sup>–Lys<sup>408</sup> is 0.45 Å.

The orientation of the peptide on the micelle surface can be postulated from analysis of the hydrophobic/hydrophilic distribution of the amino acids of the final structures. In Figure 7, the region of hydrophobic residues is highlighted. The side chains of Val<sup>384</sup>, Leu<sup>385</sup>, and Leu<sup>389</sup> are very well defined, indicating reduced conformational freedom which could result from the interaction with the surface of the micelle. In Figure 7, two arginines (Arg<sup>383</sup> and Arg<sup>390</sup>) are found on the same hydrophobic surface domain and therefore may also be in contact with the micelle; both arginines are positively charged under the experimental conditions and would favorably interact with the negatively charged SDS micelle surface.

Recently the I3 of bovine rhodopsin was studied in water by NMR, distance geometry calculations, and NOE-restrained energy minimization.<sup>45</sup> The peptide containing 22 amino acids is for the most part unstructured in aqueous solution, in accord with the observations made here. The one structural feature of the peptide is one turn of an  $\alpha$ -helix in the central portion of the peptide. Since the structure of the N-terminal 6-amino acids of the peptide is completely undetermined, the distance between the N- and C-termini cannot be calculated. From simple model building, it is concluded that the turn of  $\alpha$ -helix must be surrounded by turns (i.e., turn–helix–turn motif), so that the peptide may attach to the TM helices V and VI of the rhodopsin receptor.<sup>45</sup> These results should be contrasted with the cyclic analog studied here, in which the attachment to the TM helices has been accounted for in the design of the peptide and incorporation of the octamethylene linker.

Our current PTH/PTHrP receptor cyclic third loop mimetic construct was targeted to closely reproduce the structural constraints imposed by binding to TM helices V and VI. However, it lacks the hydrophobic features that would lead to a high membrane-associated concentration, which may be required to activate the membrane-bound G-proteins. Mastoparan contains a hydrophobic phase that may result in an effective local concentration on the membrane, leading to activation of the G-protein. However, the I3 of the PTH/PTHrP receptor cannot be modeled as an amphiphilic  $\alpha$ -helix.

(54) Ross, E. M.; Higashijima, T. *Methods Enzymol.* **1994**, *237*, 26–37.

To increase the effective concentration of the PTH/PTHrP receptor loop mimetic at the membrane, our future design will include the incorporation of lipophilic moieties such as palmitoylated or myristoylated residue at the C-terminus and possibly another at the N-terminus. The interdigitation of the long fatty-acyl chain of these end groups into a biomembrane will ensure a high concentration of the peptide at the membrane surface. A similar approach has been successfully utilized in the study of

---

(55) Moroder, L.; Romano, R.; Guba, W.; Mierke, D. F.; Kessler, H.; Delporte, C.; Winand, J.; Christophe, J. *Biochemistry* **1993**, 32, 13551–13559.

the interaction of cholecystokinin with its G-protein coupled receptor.<sup>55</sup>

**Acknowledgment.** We are grateful to the National Institutes of Health (GM-54082) for research support.

**Supporting Information Available:** A listing of the proton chemical shifts, NOEs, and distance restraints and the dihedral order parameters for the  $\phi$  and  $\psi$  torsions for both the linear and cyclic peptide in the presence of SDS micelles (11 pages). See any current masterhead page for ordering and Internet access instructions.

JA960454P